

Disorder-induced TA Raman lines in mixed Cu-halide crystals

Z. Vardeny and O. Brafman

Department of Physics and Solid State Institute, Technion—Israel Institute of Technology, Haifa, Israel

(Received 23 March 1978; revised manuscript received 30 May 1978)

The Raman spectra of $\text{CuCl}_x\text{Br}_{1-x}$ and $\text{CuBr}_x\text{I}_{1-x}$ solid solutions are shown to contain extremely intense disorder-induced first-order TA phonons. The intensity of these lines is a function of the concentration x , and is highest in $\text{CuCl}_{0.60}\text{Br}_{0.40}$. The TA spectrum, well resolved at low temperature, fits well the density of states (DOS) calculated from inelastic-neutron-scattering data. Assuming a disorder model in which Cu^+ populates the central site or off-center sites, the high-intensity of this line and its temperature and pressure dependence are explained. The Grüneisen parameters of the TA lines were measured in various mixed crystals, and fit well other related thermodynamic parameters. The low-temperature 2TA lines of both pure and mixed crystals fit the calculated two-phonon DOS. The spectral analysis at high temperature is discussed, and it is found that $\omega_{2\text{TA}}(T)$ follows nicely $2\omega_{\text{TA}}(T)$.

I. INTRODUCTION

The general properties of pure Cu-halide crystals were reviewed in the previous paper, hereafter referred to as I.¹ In that report a variety of phonon anomalies are described and interpreted. One of these anomalies relates to the weak low-frequency lines observed in the Raman spectra of the pure compounds²⁻⁴ and were briefly mentioned in I. These lines will be examined more intensely here.

This study is devoted to Cu-halide solid solutions in their zinc-blende (ZB) structure. Mixed Cu halides were studied earlier by Murahashi and Koda.^{5,6} They investigated the behavior of the $\bar{k} \approx 0$ optical phonons in Raman and infrared absorption, at low temperatures and found a two-mode behavior in⁵ $\text{CuCl}_x\text{Br}_{1-x}$ and⁶ $\text{CuCl}_x\text{I}_{1-x}$ and a one-mode behavior in $\text{CuBr}_x\text{I}_{1-x}$.⁶ Lower-frequency lines in mixed Cu halides were not reported.

The present report will deal mainly with the acoustical phonons of $\text{CuCl}_x\text{Br}_{1-x}$, and $\text{CuBr}_x\text{I}_{1-x}$, emphasizing the disorder-induced Raman lines. Only a few works on disorder-induced lines in mixed crystals were reported in the past.^{7,8} We shall demonstrate and explain the special character of this phenomenon in the mixed Cu-halide systems.

The experimental techniques are described in Sec. II and the results are reported in Sec. III. In Sec. IV the results are analyzed and discussed. The conclusions are summarized in Sec. V.

II. EXPERIMENTAL

The mixed crystals were grown using the Bridgman technique. In the case of $\text{CuCl}_x\text{Br}_{1-x}$, 5 mol% of KCl was added as a flux.^{5,6} The composition

ratios were quite uniform for all concentrations of $\text{CuCl}_x\text{Br}_{1-x}$ and $\text{CuBr}_x\text{I}_{1-x}$, while uniformity could not be obtained in $\text{CuCl}_x\text{I}_{1-x}$.

The Raman spectra were taken using a standard set up including a third Spex monochromator for a proper detection of the low-frequency Raman lines. Both 90° and back-scattering spectra were taken, using slits of about 3-cm⁻¹ effective width. Both Ar⁺ and Kr⁺ lasers were used as light sources. Immersion and cold finger type cryostats were used for the temperature range of 2–300 K. High-temperature measurements up to 300 °C were taken in an atmosphere of Ar gas. Temperature was stabilized to within ±0.5 °C at low temperature and ±2 °C at high temperatures. The hydrostatic pressure cell utilizes sapphire windows and is designed for pressures up to 10 kbars at room temperature. The pressure is measured by means of a manganin wire. A more detailed description of the pressure cell was given elsewhere.⁹

III. RESULTS

Figure 1 shows the room-temperature spectra of $\text{CuCl}_x\text{Br}_{1-x}$, $0.04 \leq x \leq 0.95$. The lower-frequency lines, which were not investigated earlier,⁵ are marked by the letters d and α . The higher-frequency part of the spectra consists of lines due to scattering from optical phonons of CuCl and CuBr.^{5,6} These lines are disregarded in the present report. It can be noticed that the d -line intensity varies with concentration and maximizes around equal mixture of the two compounds. Its peak frequency slightly shifts from 34.5 cm⁻¹ in $\text{CuCl}_{0.95}\text{Br}_{0.05}$ to 36.5 cm⁻¹ in $\text{CuCl}_{0.10}\text{Br}_{0.90}$. Very weak Raman lines are also detected in the pure compounds around the respective frequencies.¹⁻⁴ The α -line relative intensity increases gradually from CuBr to CuCl. Its frequency shifts from 70

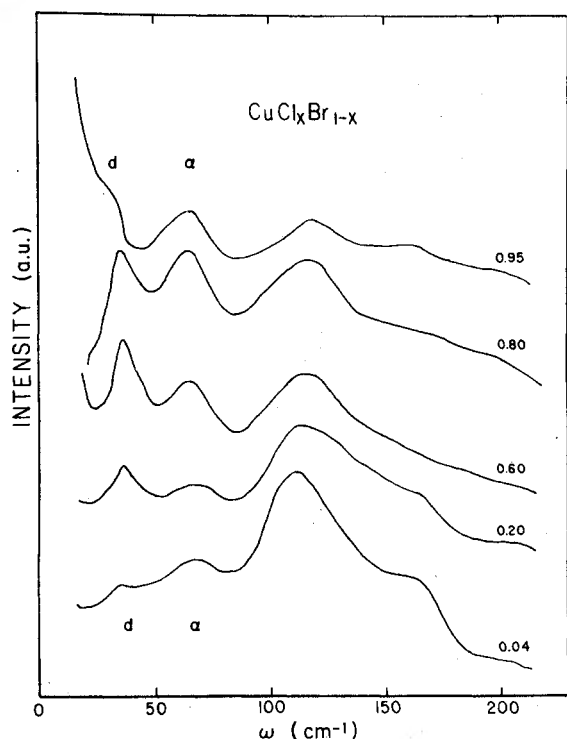


FIG. 1. Room-temperature Raman spectra of $\text{CuCl}_x\text{Br}_{1-x}$, $x=0.95, 0.80, 0.60, 0.20, 0.04$. The disorder-induced TA line (d) and the 2TA Raman-active line (α) are explained in the text. The rest of the spectrum consists of scattering from optical phonons of CuCl and CuBr (Refs. 5 and 6).

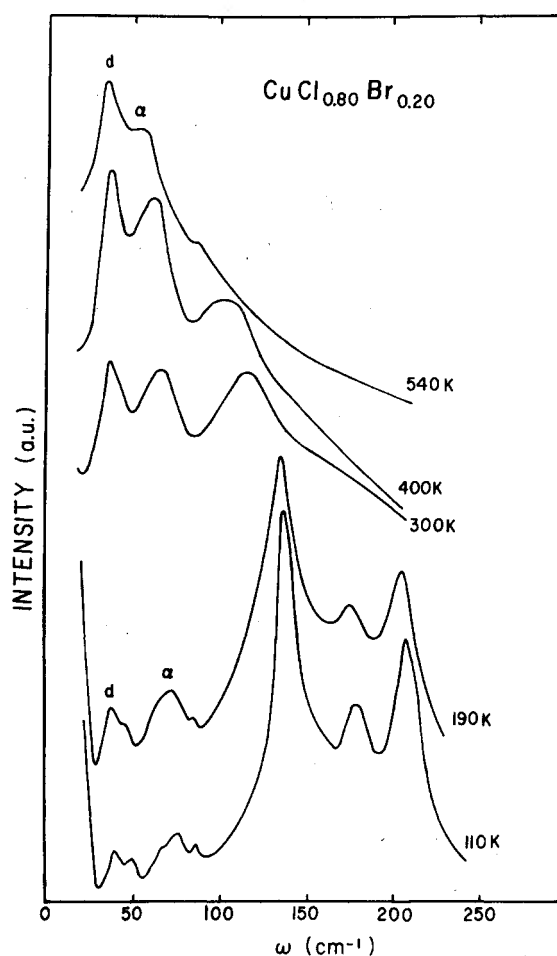


FIG. 2. Raman spectra of $\text{CuCl}_{0.80}\text{Br}_{0.20}$, at various temperatures. The lines d and α as in Fig. 1.

cm^{-1} in CuCl (Refs 4 and 10) to 75 cm^{-1} in CuBr (Refs. 2, 4, and 11). This line is a second-order Raman-active line and therefore appears in the pure materials as well.^{10,11} The broad lines of these spectra are typical also of the pure crystal spectra at room temperature.

Additional information on the d and α lines of $\text{CuCl}_{0.80}\text{Br}_{0.20}$ is obtained from the spectra at different temperatures presented in Fig. 2. $\text{CuCl}_{0.80}\text{Br}_{0.20}$ is a convenient mixture to be studied, for it properly shows the special features of the mixed Cu halides and is sufficiently close to CuCl for which comprehensive experimental data are available.⁵ The spectrum at 110 K clearly shows the splitting of the d line. Actually three lines, labeled d_0 , d , and d_1 can be observed, though the low-frequency one (d_0) is hardly resolved in the figure. Similarly, the α line splits into three well resolved lines labeled α_0 , α , and α_1 . At high temperature we refer to the unresolved lines as d or α lines labeled after the most intense line of its group. It should be noted that also the optical phonon spectrum is better defined at 110 K. Figure

2 demonstrates the enhancement of the d and α lines with temperature beyond that of the optical phonon lines.

Figure 3 shows the room-temperature spectra of $\text{CuCl}_{0.60}\text{Br}_{0.40}$ at 1 bar and at 9 kbars. The main difference between these two spectra is the weakening of the d line with pressure, which holds in all the mixed Cu halides.

Figure 4 presents the room-temperature Raman spectra of $\text{CuBr}_x\text{I}_{1-x}$, $x=1, 0.80, 0.50, 0.20, 0$. The d and α lines are indicated in the figure. When the d -line intensity is compared with the intensity of the other lines of the same spectrum, it is clear that its relative intensity in a crystal with high bromine concentration is larger than that in a crystal with high iodine concentration.

The room-temperature shifts under pressure of the d lines were measured in the following

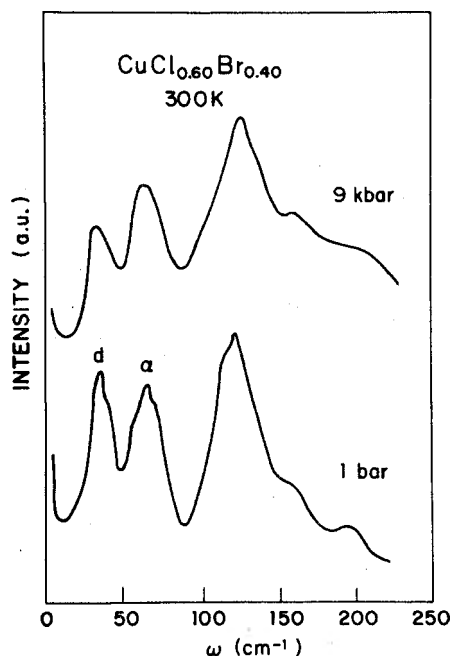


FIG. 3. Room-temperature Raman spectra of $\text{CuCl}_{0.60}\text{Br}_{0.40}$ at atmospheric pressure and at 9 kbars.

crystals: $\text{CuCl}_{0.80}\text{Br}_{0.20}$, $\text{CuCl}_{0.20}\text{Br}_{0.80}$, $\text{CuBr}_{0.20}\text{I}_{0.80}$ and pure CuI. The accepted value is an average of eight different measurements on each crystal at around 8 kbars. In order to evaluate the mode Grüneisen parameters

$$\gamma_j = \frac{1}{\chi_T \omega_j} \frac{d\omega_j}{d\rho}$$

the isothermal compressibility χ_T was linearly interpolated from the known values of the pure crystals. $\chi_T = 2.63, 2.56, 2.81$ ($10^{-3}/\text{kbar}$) for CuCl, CuBr, and CuI, respectively.¹² The d -mode Grüneisen parameters were found to be $\gamma(\text{CuCl}_{0.80}\text{Br}_{0.20}) = -1.4$, $\gamma(\text{CuCl}_{0.20}\text{Br}_{0.80}) = -0.4$, $\gamma(\text{CuBr}_{0.20}\text{I}_{0.80}) \approx \gamma(\text{CuI}) \approx 2.5$. We are not concerned here with the accurate γ values; the important part of these results is that for high concentration of CuCl $\gamma < 0$, it is smaller but still negative for high concentration of CuBr, while $\gamma > 0$ for the d line of CuI.

IV. DISCUSSION

The discussion is divided into two main parts. In the first one the assignment of the d line as a disorder-induced TA is justified. The unusual high intensity of the d line together with its temperature and pressure dependence is explained according to the model presented in I. The second part is devoted to the α line and its assignment as 2TA

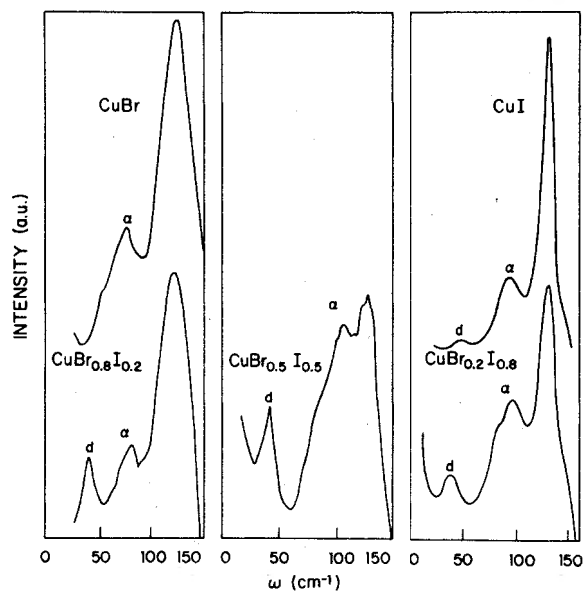


FIG. 4. Room-temperature Raman spectra of $\text{CuBr}_x\text{I}_{1-x}$, $x=0, 0.20, 0.50, 0.80, 1$. The d and α lines as in Fig. 1. The rest of the spectra consists of scattering from optical phonons (Refs. 5 and 6).

and to a general analysis of the spectra at high temperatures.

A. d line

In pure Cu halides a reminiscence of an extra line at low frequencies is detected at room temperature.²⁻⁴ This line was resolved in CuCl (see I) and CuI (Fig. 4); in CuBr it appears as a tail at the low-frequency side of the α line (Fig. 4 and I). The assignment of the d line is not straightforward: it may approximately fit LO-TA at X , L , or K critical points in CuBr,⁴ but not in CuI,²⁻⁴ or CuI.²⁻⁴ The intensity of the d line is too weak for measuring its temperature or pressure dependence. On the other hand, the frequencies of these lines do fit the TA frequencies at the zone-boundary symmetry points measured by inelastic neutron scattering at 300 K.¹³⁻¹⁷ The α lines appear at twice these frequencies in the respective compounds.^{2,4,10,11} This hints that the d lines might be first-order TA Raman lines. Such a conclusion may be valid only if a TA line is disorder induced, for otherwise it is ruled out because of the \vec{k} -conservation selection rule. From I it can be inferred what might be the mechanism of such a disorder or a short correlation length. The experimental support for this approach can be found in increasing the amount of disorder and examining its effect on the d line intensities. Indeed, Fig. 1

demonstrates the striking enhancement of the d -line intensity in mixed $\text{CuCl}_x\text{Br}_{1-x}$ and its dependence on the concentration x . A similar effect is shown in Fig. 4 for the mixed $\text{CuBr}_x\text{I}_{1-x}$. Thus we conclude that the d lines are disorder-induced first-order TA phonons originating from the zone boundary in various symmetry directions. Moreover, the temperature-dependent frequency of the d lines is the same as that extrapolated from neutron scattering of the TA critical-point frequencies of the pure crystals.¹³⁻¹⁷ We shall see later that it fits also half the frequency of the respective α lines.

In support of the conclusion that the d lines are zone boundary TA phonons, the following studies were performed: (i) a careful examination was made of the Raman d lines and their relation to the one-phonon density of states, calculated from the phonon dispersion relations.¹³ (ii) The d -lines pressure-induced frequency shifts measured in several mixed crystals were compared with the expected TA critical-point phonon frequency shifts in the pure materials.

(i) In all the mixed Cu-halide crystals when cooled down, three peaks are resolved around the respective d -line frequencies (it is demonstrated for $\text{CuCl}_x\text{Br}_{1-x}$ in Fig. 2). We claim that these peaks labeled d_0 , d , and d_1 are $\text{TA}(L)$, $\text{TA}(X)$, and $\text{TA}(K)$, respectively. In order to prove this assignment, the one-phonon density of states (DOS) was calculated.

A simple shell model¹⁸ using seven disposal parameters was fitted to the room-temperature phonon dispersion relations of CuCl measured by inelastic coherent neutron scattering.¹³ The repulsive interactions were described by two force constants (A and B) for nearest neighbors and only two central force constants for next-nearest neighbors: A' (Cu) for Cu-Cu and A'' (Cl) for Cl-Cl.¹⁹ For the more polarizable ion (Cl^-), shells with effective charges e_y and force constants k connecting them to their inner ionic cores, were assigned. The Coulomb interaction was taken into account introducing the effective charges $-ez$ on the Cl^- and $+ez$ on the Cu^+ . A good fit was obtained especially for the acoustical branches in which we are more interested. The best seven parameters obtained are given in Table I. These parameters

TABLE I. Best-fit parameters of the shell model used to calculate $\omega_j(\vec{k})$ and $g(\omega)$ for CuCl. The parameters are given in units of $e^2/2V_0$, where V_0 is the unit-cell volume.

Z	Y (Cl)	k (Cl)	A	B	A' (Cu)	A'' (Cl)
0.45	-1.5	32.4	9.6	9.5	0.8	-1.7

were used to calculate the density of states (DOS) $g(\omega)$ with the aid of the extrapolation method,²⁰ using 2992 crude mesh cubes uniformly distributed over $\frac{1}{24}$ of the first Brillouin zone. The same method was used to calculate the two-phonon density of states $g_2^+(\omega)$ (sum) and $g_2^-(\omega)$ (difference). Figure 5 demonstrates the excellent fit between the calculated DOS of pure CuCl and the low-temperature experimental Raman spectrum of $\text{CuCl}_{0.80}\text{Br}_{0.20}$. This means that the TA polarizability is similar in the various symmetry directions. Since the DOS was obtained in pure CuCl at 300 K, while the experimental spectrum is that of $\text{CuCl}_{0.80}\text{Br}_{0.20}$ at 110 K, a slight difference in the line frequencies is expected and is observed.

From the inelastic neutron scattering data at room temperature¹³ the TA frequencies at L , X , and K critical points, are 31, 33, and 44 cm^{-1} , respectively in CuCl, while they are 31, 36, and 50 cm^{-1} in CuBr.^{15,16} In CuCl, at 4.2 K,¹⁴ these frequencies shift to 33, 38, and 49 cm^{-1} . Therefore about 1, 4, and 5 cm^{-1} should be subtracted, respectively, from the frequencies of d_0 , d , and d_1 lines, when compared to the room-temperature DOS of CuCl TA at L , X , and K critical points. On the other hand, the calculated two-phonon difference DOS [$g_2^-(\omega)$] shown also in Fig. 5, does not have any resemblance to the experimental

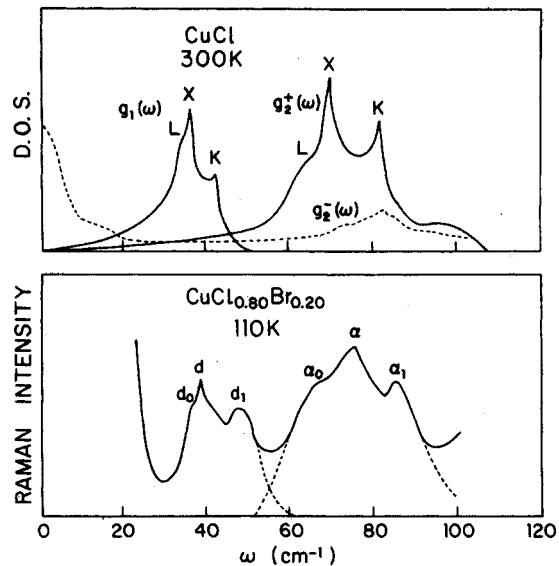


FIG. 5. Raman spectrum of $\text{CuCl}_{0.80}\text{Br}_{0.20}$ at 110 K, compared with the calculated density of states (DOS) at 300 K of one-phonon [$g_1(\omega)$], two-phonon sum DOS [$g_2^+(\omega)$], and two-phonon difference DOS [$g_2^-(\omega)$]. The scales for $g_1(\omega)$ and $g_2^-(\omega)$ are different and were chosen to fit the intensity of the experimental d and α spectra.

d-line spectrum.

From the inelastic neutron scattering data,¹³⁻¹⁷ it is clear that the TA branches of CuCl, CuBr, and CuI look very much alike. Therefore, it is expected that the TA phonon branches will exhibit a one-mode behavior in their mixtures.

(ii) The measured pressure-induced frequency shifts of the *d*-lines main peak yield a negative mode Grüneisen parameter for CuCl, smaller but still negative for CuBr and a positive value for CuI. In CuCl it was found²¹ that both shear elastic constants decrease with pressure, which implies that the TA mode Grüneisen parameter should be negative. No such measurements were performed on CuBr and CuI. The thermal-expansion coefficients of CuCl,^{22,23} and CuBr,²³ become negative at low temperatures, which suggests $\gamma(\text{TA}) < 0$ in these compounds. On the other hand, the thermal-expansion coefficient of CuI stays positive at all temperatures.²³ It is possible²⁴ to measure directly $\gamma(\text{TA})$ in the other phases of CuI, obtained by the application of high hydrostatic pressure: The cubic (ZB) TA(L) becomes Raman active in the rhombohedral phase which is explained by the folding of the zinc-blende Brillouin zone in the [111] direction; $\gamma > 0$ was obtained for this mode.²⁴ The ZB TA(X) becomes Raman active in the tetragonal phase (folding in the [100] direction) and again $\gamma > 0$ was obtained for this mode.²⁴ From the extrapolation of the frequencies under pressure, a conclusion may be reached that $\gamma(\text{TA}) > 0$ also in the ZB structure.²⁴ This is consistent with the present result obtained on the *d* lines of CuI and CuBr_{0.20}I_{0.80}. Also a good fit is obtained between the experimental mode Grüneisen parameter of the *d* line in CuCl_{0.80}Br_{0.20}, which is -1.4 and the elastic Grüneisen constant γ_{elastic} , calculated by Hanson *et al.*²¹ at room temperature, which is -1.17.

In the above discussion the assignment of the *d* lines as disorder-induced first-order Raman lines originating from TA at critical points was established. Yet, two questions remain: Why are the *d*-line intensities unusually high and is the intensity temperature dependence that of a first-order Raman line?

To be convinced that the high intensity of the *d* line is anomalous, it should first be compared with disorder-induced lines in other compounds. Indeed, in all the mixed crystals where acoustic disorder-induced Raman lines were detected,^{7,8} these lines were found to be very weak. An example is given in Fig. 6 showing the room-temperature Raman spectrum of ZnS_{0.50}Se_{0.50}. TO₁ and LO₁ are the optical phonon lines of ZnSe and TO₂ and LO₂ are those of ZnS. α are second-order Raman lines.²⁵ The disorder-induced TA line is around 70–90 cm⁻¹ where it

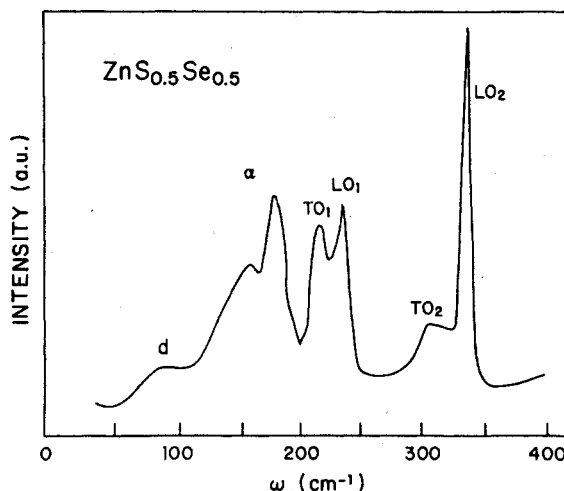


FIG. 6. Room-temperature Raman spectrum of ZnS_{0.50}Se_{0.50}. The line *d* is a disorder-induced TA band (Ref. 26). The α lines are due to second-order scattering process. TO₁, TO₂, LO₁, and LO₂ are optical-phonon lines; 1 is related to ZnSe lines and 2 to ZnS lines (Ref. 25).

ought to be,²⁶ but its intensity is rather weak relative to the rest of the Raman lines. On the other hand, in CuCl_{0.60}Br_{0.40} (Fig. 1) the respective line is the most intense Se Raman line of the entire spectrum.

The intensity temperature dependence of the *d* lines in mixed Cu halides does not follow the behavior of a first-order Raman line, nor that of a two-phonon difference line. The high intensity and its complex temperature dependence can be understood on the basis of the dynamical model presented in I.

It is proposed that in pure Cu-halide crystals, Cu⁺ ions may occupy their ideal positions or four equivalent off-center sites in the [111] directions, toward the faces of the tetrahedra formed by the anions.¹ The off-center Cu⁺ population is temperature and pressure dependent via $\Delta(T, P)$, the energetic difference between off-center and center potential wells, which in turn depends on the lattice constant $a(T, P)$.¹ How this affects the optical phonons is described in length in I. With regard to the acoustical phonons, the off-center Cu⁺ ions act as phonon scattering centers, namely, these ions may introduce disorder, which relaxes the selection rules and may yield new lines in the Raman spectrum.

In order to describe phonon waves in disordered crystals, it is useful to introduce mode correlation length $\Lambda(Q_j)$ (see Refs. 27 and 1). This will result in a decay of the spatial correlation func-

tion²⁷:

$$R(\vec{r}, Q_j) = A(Q_j) \exp(i\vec{k}_j \cdot \vec{r}) \exp[-|\vec{r}|/\Lambda(\vec{k}_j)]. \quad (1)$$

The Raman intensity scattered from the mode Q_j is proportional to the Fourier transform of $R(\vec{r}, Q_j)$:

$$I(\vec{k}_j) \propto \Lambda_j^3 / (1 + \vec{k}_j^2 \Lambda_j^2)^2. \quad (2)$$

The total Stokes scattered intensity is obtained by integration:

$$I(\omega) \propto \int_{\text{BZ}} I(\vec{k}_j) \frac{n(\omega) + 1}{\omega} \delta(\omega - \omega(\vec{k}_j)) d^3k, \quad (3)$$

where $n(\omega)$ is the Bose-Einstein occupation number.

In proper crystals, Λ_j are high enough and $I(\vec{k}_j)$ is a δ function centered around $\vec{k}_j \approx 0$. When Λ_j decreases, the conservation of momentum relaxes and modes with $\vec{k}_j \neq 0$ also contribute to the scattered intensity. It is then expected to find peaks in $g(\omega)$ (DOS) on top of the regular $\vec{k} \approx 0$ Raman spectrum.²⁷

In the case of Cu halides the TA branches are relatively flat giving rise to very intense peaks in $g(\omega)$ at the TA critical-point frequencies. The off-center Cu ions lower the correlation length and new lines in the Raman spectrum, which correspond to these peaks in $g(\omega)$ are due. This explains the relatively weak d lines in pure Cu-halide room-temperature spectra.

When a partial substitution of the anions is made by introducing a different type of halogen, the correlation length of the TA phonons decreases further. But the mixing of the anions also induces a greater disorder of the off-center Cu ions. In pure Cu-halide crystals the four off-center potential wells were equivalent,¹ while this is no longer true in the mixed Cu halides. Thus the disorder caused by the anionic mixture is therefore larger than that in the common mixed crystals. However, disorder-induced Raman lines due to the LA, TO, and LO peaks in the DOS are not detected. As stated before the disorder-induced TA lines are expected to be more intense and indeed in CuI when the TA(L) and TA(X) become Raman active under phase transformation to rhombohedral and tetragonal phases, respectively, these lines are by far the most intense lines of the Raman spectra.²⁴ The Raman-active optical phonon lines of the mixed crystals are very broad at room temperature^{5,6} and weak disorder-induced lines cannot be observed in this frequency range. At low temperatures when the Raman lines are better defined, the cationic disorder is drastically reduced in the mixed crystals, because of the decrease in the off-center Cu⁺ population on cooling, as explained in I.

The intensity temperature dependence of the d lines is explained in the same fashion. At lower temperature, on top of the $n+1$ first-order Raman factor, the decrease in the off-center Cu⁺ population reduces the amount of disorder and thus causes an additional decrease in the Raman intensity of the d lines. We shall return to this factor later when the temperature dependence of the TA and 2TA lines will be dealt with. In addition to the temperature dependence, also the intensity pressure dependence of the d lines was measured. It was proposed in I that the application of pressure, which decreases the lattice parameter, reduces the off-center Cu⁺ population and therefore the TO(β) intensity of CuCl decreases.²⁸ But the decrease in the off-center Cu⁺ population should also weaken the d -line intensity and this is indeed what happens! It can be seen in Fig. 3 that while the intensity of the other lines hardly changes when pressure of 9 kbars is applied, the decrease in the d -line intensity is remarkable.

It has been shown in I that going from CuCl to CuI a trend is found in respect to the phonon anomalies, which follows the same course deduced from the Bragg intensity temperature dependence of x-ray and neutron scattering. Both stem from the off-center Cu⁺ population being important even at low temperatures in CuCl, at higher temperatures in CuBr and only above room temperature in CuI. A respective trend is also found for the d -line observation in the mixed crystals. We were able to detect the d line in CuCl_{0.80}Br_{0.20} even at 50 K, the d line in CuCl_{0.20}Br_{0.80} at 100 K and that of CuBr_{0.20}I_{0.80} disappeared at 150 K.

The intensities of the d lines in the various mixtures can be compared in a qualitative manner. In spite of the higher polarizabilities going from Cl⁻ to I⁻, the intensities of the d lines relative to the respective spectra seem to decrease in the following sequence: CuCl_{0.80}Br_{0.20}, CuCl_{0.20}Br_{0.80}, CuBr_{0.80}I_{0.20}, CuBr_{0.20}I_{0.80}.

B. α line

The α line is observed in all Cu-halide Raman spectra as well as in all Cu-halide solid solutions. In several reports^{2,10,11} it was assigned as TO-TA at various critical points, in other reports it was assigned as 2TA without verification.²⁹ As a matter of fact, not only the TO-TA assignment but also any other two-phonon difference assignment of the α line in CuCl is unfounded. This can be clearly concluded from the comparison of the Raman spectrum with the calculated two-phonon difference DOS shown in Fig. 5. The fact that this line is observed even at 2 K, both in Raman^{5,6,30} and in infrared absorption,²⁹ rules out the possibility of a difference combination. Similarly

to the d line, the α line splits at low temperature and can be compared to the two-phonon DOS. Figure 5 shows an excellent fit between the Raman spectrum at 110 K and the calculated two-phonon summation DOS $g_2^+(\omega)$ at 300 K. The slight frequency differences are due to the different temperatures. We believe that this fit does not leave much doubt about the assignments of α as 2TA (there is no noticeable difference between the α line in pure CuCl and $\text{CuCl}_{0.80}\text{Br}_{0.20}$). However, at elevated temperature the observed α -line frequency deviates from twice the frequency of d (\equiv TA) (see Fig. 2). This deviation is understood from a more general analysis of Raman spectra at high temperature.

Stokes first-order Raman intensity is³¹

$$I(\omega) \propto [n(\omega) + 1]S(\omega), \quad (4)$$

where $n(\omega) = [\exp(\hbar\omega/kT) - 1]^{-1}$ is the Bose-Einstein occupation number at a given temperature T and $S(\omega)$ is the spectral density function of the dielectric functions at $\vec{k} \approx 0$. Similarly, for a second-order combination one obtains

$$I(\omega) \propto [n(\omega/2) + 1]^2 S(\omega). \quad (5)$$

The function of interest is $S(\omega)$ which is obtained from the experimental spectrum dividing it by $[n(\omega) + 1]$ or by $[n(\omega/2) + 1]^2$ for first- and second-order Raman lines, respectively. At high temperatures ($\hbar\omega \ll kT$), the respective factors are ω^{-1} and $(\omega/2)^{-2}$. At low temperatures the reduced spectrum $S(\omega)$ and the recorded one $I(\omega)$ look alike, but dramatic changes may occur at high temperatures, where the temperatures parameters may distort the phonon spectrum.

Normally, for narrow phonon lines this will not happen, but in anharmonic crystals where the Raman spectrum consists of very broad lines, a careful analysis is required at high temperatures.³¹ This is the case in Cu halides.

The CuCl Raman spectrum at room temperature is chosen for demonstrating the results of such an analysis, namely, the reduced Raman spectra. In order to obtain the reduced spectrum at room temperature, the Raman spectrum is subdivided into the α Lorentzian and the rest of the spectrum, which consists of the higher-frequency optical phonon lines (see Fig. 7). Then the α part is treated as second order (2TA), while the higher-frequency part is treated as if it were a normal first-order Raman. Figure 7 shows the changes induced in the intensities, the resolution and the frequencies when the reduced spectrum is obtained. The α line becomes less intense than the α and α_1 optical lines. It is then resolved to α and α_1 similarly to the lower-temperature spectrum. It shifts to higher frequency [from 65 cm^{-1} in the

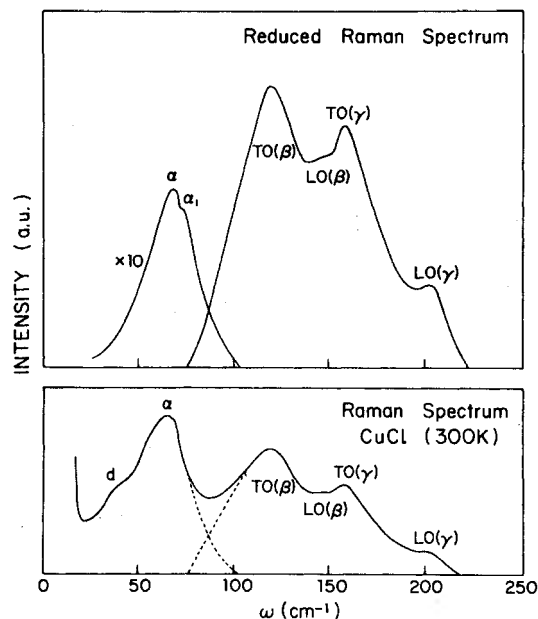


FIG. 7. Raman spectrum and the reduced spectrum (see text) of CuCl at 300 K. Note the difference in scale in the reduced spectrum; the low-frequency intensity unit is 10 times smaller than that of the high-frequency one. TO(β), LO(β), TO(γ), and LO(γ) are optical phonons and are explained in length in I (Ref. 1).

Raman spectrum to 70 cm^{-1} in the reduced one ($\Delta\omega = 5 \text{ cm}^{-1}$). The respective changes in the optical lines are minor, except for the fact that the reduced spectrum now resembles the lower-temperature Raman spectrum. At higher temperatures, isolating the α Lorentzian from the rest of the spectrum becomes more difficult and the approximation made for the optical lines becomes poorer. However, since we are interested mainly in the α lines, this procedure can still be considered a good approximation for resolving the quasiharmonic α frequencies. Thus the frequency shifts ($\Delta\omega$) of α between the Raman spectrum and the reduced spectrum can be measured. The values of $\Delta\omega$ of α in CuCl as function of temperature are given in Table II.

TABLE II. Frequency shift $\Delta\omega$ between the α experimental Raman frequency and its reduced spectrum frequency, at various temperatures.

T (K)	100	200	300	400	500	600
$\Delta\omega$ (cm^{-1})	1	3	5	8	12	16

The same procedure was applied to all the pure and mixed Cu halide spectra. Table III gives the d and α lines frequencies obtained from the room-temperature spectra of $\text{CuCl}_x\text{Br}_{1-x}$ for various x concentrations. In most of the cases all the lines of the low-temperature spectra are resolved in the reduced spectra. Only in two cases the weak lines were not resolved. We shall concentrate now on the analysis of $\text{CuCl}_{0.80}\text{Br}_{0.20}$ in order to have some insight into the approximations made and the conclusions reached.

Unlike the pure CuCl , the spectrum of $\text{CuCl}_{0.80}\text{Br}_{0.20}$ contains an intense d line at high temperature (see Fig. 2). This d line being a well defined Raman line does not show any frequency shift ($\Delta\omega$) when compared with the reduced spectrum. (Its intensity becomes weaker in the reduced spectrum.) The shift $\Delta\omega$ of α obtained at each temperature was the same as that obtained earlier in CuCl . In the reduced spectra the three lines α_0 , α , and α_1 are resolved and Table IV shows the excellent fit between $\omega(\alpha_0)$, $\omega(\alpha)$, and $\omega(\alpha_1)$ and $2\omega(d_0)$, $2\omega(d)$, and $2\omega(d_1)$ respectively, at the various temperatures. This further supports the assignment of the d lines as first-order Raman lines and the assignment of the α lines as their respective harmonics.

In order to check the consistency of the whole technique an attempt was made to reproduce the Raman spectrum of $\text{CuCl}_{0.80}\text{Br}_{0.20}$ at 540 K starting from the 110-K spectrum, where all the Raman lines are well separated. The intensity of each Lorentzian observed at the 100-K spectrum is multiplied by the suitable factor, according to whether it is a first- or second-order process. When the temperature-dependent frequency and the temperature-induced broadening are considered, the 540-K Raman spectrum can be well reproduced, except for the d line, the intensity of which is then too low. This procedure clarifies that the d -line intensity exhibits a larger than $n+1$ dependence. This is consistent with the previous subsection A, where it is also explained.

TABLE III. Room-temperature frequencies of the d and α lines of the reduced spectra of $\text{CuCl}_x\text{Br}_{1-x}$. The frequencies are given in units of cm^{-1} .

X	d_0	d	d_1	α_0	α	α_1
0.95	30.5	34.5			71	77
0.80	31	35	41	64	71	79
0.60	32	35.5	42	66	72	80
0.20	32.5	36	42	67	72	81
0.10		36	44	68	73	83
0.04	33	36.5	46	70	74	

V. SUMMARY

The intense d lines, which appear in the Raman spectra of mixed Cu halides, are assigned as TA disorder-induced vibrations at L , X , and K critical points. The three lines are well resolved at low temperatures. This assignment is based on the following facts: (i) their intensity depends on the concentration of the mixture and maximizes around equal concentration of the anions involved. (ii) The frequencies fit those obtained from inelastic neutron scattering for the TA at critical points. (iii) When compared to the calculated one-phonon DOS, an excellent fit is obtained. Moreover, the two-phonon DOS either $g_2^+(\omega)$ or $g_2^-(\omega)$ have no peak in this frequency region. (iv) The d -mode Grüneisen parameters measured in $\text{CuCl}_{0.80}\text{Br}_{0.20}$, $\text{CuCl}_{0.20}\text{Br}_{0.80}$, and $\text{CuBr}_{0.20}\text{I}_{0.80}$ fit those expected in the pure CuCl , CuBr , and CuI , respectively.

On the other hand, the intensity temperature dependence does not follow the behavior of a first- or that of a second-order process. The model presented in I accounts for this temperature dependence as well as for the unusual high intensity of these lines and its weakening with pressure. In the case of mixed Cu halides this model requires that Cu^+ may populate off-center sites or central position. Because of the anionic mixture, an additional disorder of the off-center copper ions is induced. Thus the relaxation of the k selection rule arises from three sources: the short correlation length due to off-center Cu^+ , due to the anionic mixture and the disorder this mixture induces on the off-center Cu^+ . The intense DOS peaks at the TA branches and the high degree of disorder cause these lines to be more intense than previously observed in other solid solutions.

The temperature and pressure dependence of the off-center Cu^+ population is reflected in the intensity. Therefore, the disorder TA intensity diminishes at low temperature and high pressure,

TABLE IV. Temperature-dependent frequencies of d and α lines of the $\text{CuCl}_{0.80}\text{Br}_{0.20}$ reduced spectra. The frequencies are given in units of cm^{-1} .

T (K)	d_0	d	d_1	α_0	α	α_1
110	34.5	38	48	68	75	89
190	34.5	37	46	67	74	87
250	33	36	43	66	73	83
300	31	35	41	64	71	79
350	31	34.5	40		70	79
400	30	34.5	40	63	69	78
470	29.5	34	38	60	68	77
540		33		59	66	75

which corresponds to lower off-center Cu^+ population. The lowest temperature at which the d Raman line can still be detected depends on the particular anions in the mixture. In spite of the higher polarizability on going from chlorine to iodine, the dominating factor is that of the off-center Cu^+ population and in mixtures with high chlorine concentration the d line is detected at the lowest temperatures. This trend is in line with the trend found in pure Cu halides as explained in I.

The α lines, which are Raman and infrared active, are observed as well in the pure Cu-halide spectra at 2 K and are assigned to be 2TA at critical points. At low temperature, three lines are resolved at frequencies which correspond to the frequencies of 2TA at L , X , and K critical points. Again the fit to the $g_2^+(\omega)$ calculated from the phonon dispersion relations is remarkable. At higher temperatures, when the reduced spectra

line frequencies are considered, the fit to twice the TA frequencies is preserved. This supports both the assignments of TA and of 2TA.

ACKNOWLEDGMENTS

We wish to thank Dr. S. Suga for supplying the $\text{CuCl}_x\text{Br}_{1-x}$ crystals and to M. Mor for growing the $\text{CuBr}_x\text{I}_{1-x}$ crystals. Thanks are due to H. Katz for most valuable technical assistance. Many useful discussions with Professor R. Beserman are highly appreciated. The initial stage of this work was performed at Max Planck Institute, Stuttgart. One of us (O.B.) is indebted to Professor M. Cardona for his most kind hospitality. This work was submitted by one of the authors (Z.V.) in partial fulfillment of the requirements for the Ph.D thesis at the Physics Department, Technion-Israel Institute of Technology, Haifa, Israel.

-
- ¹Z. Vardeny and O. Brafman, preceding paper, Phys. Rev. B **19**, 3276 (1979), hereafter referred to as I.
- ²J. E. Potts, R. C. Hanson, and C. T. Walker, Solid State Commun. **13**, 389 (1973).
- ³G. Burns, F. M. Dacol, and M. W. Shafer, Solid State Commun. **24**, 753 (1977).
- ⁴B. Prevot, Ph. D. thesis (Strasbourg, 1971) (unpublished).
- ⁵T. Murahashi and T. Koda, Solid State Commun. **13**, 307 (1973).
- ⁶T. Murahashi and T. Koda, J. Phys. Soc. Jpn. **40**, 747 (1976).
- ⁷H. Kawamura, R. Tsu, and L. Esaki, Phys. Rev. Lett. **29**, 1397 (1972).
- ⁸J. S. Lannin, Phys. Rev. B **16**, 1510 (1977).
- ⁹O. Brafman, S. S. Mitra, R. K. Crawford, W. B. Daniels, C. Postmus, and J. R. Ferraro, Solid State Commun. **7**, 449 (1969).
- ¹⁰J. E. Potts, R. C. Hanson, C. T. Walker, and C. Schwab, Phys. Rev. B **9**, 2711 (1974).
- ¹¹E. M. Turner, I. P. Kaminow, and C. Schwab, Phys. Rev. B **9**, 2524 (1974).
- ¹²R. C. Hanson, J. R. Hallberg, and C. Schwab, Appl. Phys. Lett. **21**, 490 (1972).
- ¹³C. Carabatos, B. Hennion, K. Kunc, F. Moussa, and C. Schwab, Phys. Rev. Lett. **26**, 770 (1971).
- ¹⁴P. Prevot, B. Hennion, and B. Dorner, J. Phys. C **10**, 3999 (1977).
- ¹⁵B. Prevot, C. Carabatos, and C. Schwab, Solid State Commun. **13**, 1725 (1973).
- ¹⁶S. Hoshino, Y. Fujii, J. Harada, and J. D. Axe, J. Phys. Soc. Jpn. **41**, 365 (1976).
- ¹⁷B. Hannion, F. Moussa, B. Prevot, C. Carabatos, and C. Schwab, Phys. Rev. Lett. **28**, 964 (1972).
- ¹⁸R. A. Cowley, W. Cochran, B. N. Brockhouse, and A. D. B. Woods, Phys. Rev. **131**, 1026 (1962).
- ¹⁹Z. Vardeny, G. Gilat, and D. Moses, Phys. Rev. B (to be published).
- ²⁰G. Gilat and L. J. Raubenheimer, Phys. Rev. **144**, 390 (1966).
- ²¹R. C. Hanson, K. Helliwell, and C. Schwab, Phys. Rev. B **9**, 2649 (1974).
- ²²T. H. K. Barron, J. A. Birch, and G. K. White, J. Phys. C **10**, 1617 (1977).
- ²³H. P. Schaaake, quoted by N. Plendl and L. C. Mansur, Appl. Opt. **11**, 1194 (1972).
- ²⁴O. Brafman, M. Cardona, and Z. Vardeny, Phys. Rev. B **15**, 1081 (1977).
- ²⁵O. Brafman, I. F. Chang, G. Lengyel, S. S. Mitra, and E. Carnall, Jr., Phys. Rev. Lett. **19**, 1120 (1967).
- ²⁶L. A. Feldkamp, D. K. Steinman, N. Vagelatos, J. S. King, and G. Venkataraman, J. Phys. Chem. Solids **32**, 1573 (1971).
- ²⁷R. Shuker and R. W. Gammon, *Proceedings of the International Conference on Light Scattering in Solids, Paris, 1971*, edited by M. Balkanski (Flammarion, Paris, 1971), p. 334.
- ²⁸M. L. Shand and R. C. Hanson, *Proceedings of the International Conference on Lattice Dynamics, Paris, 1977*, edited by M. Balkanski (Flammarion, Paris, 1978), p. 115.
- ²⁹M. Ikezawa, J. Phys. Soc. Jpn. **35**, 309 (1973).
- ³⁰T. Fukumoto, S. Nakashima, K. Tabuchi, and A. Mitsuishi, Phys. Status Solidi **73**, 341 (1976).
- ³¹M. J. Delaney and S. Ushioda, Solid State Commun. **19**, 297 (1976).